Restoration of Minute Light Emissions Observed by Streak Camera Based on N-CUP Method

Masahiro Tsumori, Shinichiro Nagai, Ryosuke Harakawa, Toru Sasaki and Masahiro Iwahashi
Department of Electrical, Electronics and Information Engineering, Nagaoka University of Technology,
Nagaoka, Niigata, Japan.
E-mail: {tsumori, snagai}@stn.nagaokaut.ac.jp, {sasakit, harakawa, iwahashi}@vos.nagaokaut.ac.jp

***Abstract*—To observe high-speed phenomena such as discharge plasma, it is necessary to restore minute light emissions from an image observed by a streak camera, which includes multiple light emissions at each time. There has been proposed CUP method for restoring minute light emissions via a compressed sensing scheme; however, there is a case in which artefacts occur in the restoration results depending on initial values of the optimization for restoration. To overcome this limitation, N-CUP method that enables successful restoration of minute light emissions is proposed in this paper. N-CUP method estimates initial values suitable for the optimization by iteratively performing CUP method. Through simulation using image datasets emulating phenomena of fundamental light emissions, it was confirmed that N-CUP method obtained successful restoration results.**

I. Introduction

In the physics research, it is important to capture high-speed phenomena such as discharge plasma at ultra fast imaging speed. However, it is difficult to observe such high-speed phenomena due to the limit of frame rates of a camera using CCD or CMOS technologies.

To overcome this difficulty, ultra fast imaging techniques has been proposed [1]–[8]. Recently proposed methods [9], [10] have enabled the ultra fast imaging for objects by using specialized active illumination. Although the specialized active illumination works well for the objects, these methods cannot be applied to observe phenomena of light emissions such as discharge plasma.

To solve this problem, compressed ultrafast photography (CUP) [11] method, which does not need the specialized active illumination, has been proposed. This method acquires an observed image including multiple light emissions using a streak camera and restores minute light emissions of each time on the basis of a compressed sensing scheme, two-step iterative shrinkage/thresholding (TwIST) algorithm [12]. However, there is a case in which artefacts occur in the restoration results depending on initial values of the optimization for restoration.

In this paper, we propose a new method called N-CUP method to overcome this difficulty. N-CUP method iteratively performs the restoration process while estimating suitable initial values. First, by applying a TwIST algorithm to random initial values, we obtain the restored images. Then, by setting suitable initial values estimated from the obtained images as new initial values, we repeatedly perform the TwIST algorithm. By repeatedly generating the restored images unlike conventional method [11], N-CUP method enables to reduce the artefacts and accurately restore the shape of a phenomenon. Simulation results using image datasets emulating phenomena of fundamental light emissions show that results of restoration by N-CUP method are quantitatively and qualitatively superior than those by comparative methods.

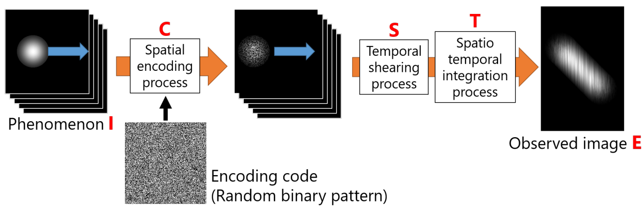

Fig. 1. Formulation of image acquisition process.

II. Restoration of Minute Light Emissions via N-CUP Method

A. Formulation of Image Acquisition Process

As shown in Fig. 1, a phenomenon $\boldsymbol{I} \in \mathbb{R}^{N_x \times N_y \times N_t}$ (N_x and N_y being the numbers of spatial coordinates; N_t being the number of temporal resolution) is changed to an observed image $\boldsymbol{E} \in \mathbb{R}^{N_x \times (N_y + N_t)}$ through the spatial encoding process, the temporal shearing process and the spatio temporal integration process. First, phenomenon $\boldsymbol{I}$ is encoded with a random binary pattern. The spatial encoding process is denoted by an operator $\boldsymbol{C} \in \mathbb{R}^{N_x \times N_y}$, and the encoded phenomenon is mathematically equivalent to $\boldsymbol{CI}$. Next, the encoded phenomenon $\boldsymbol{CI}$ temporally disperses along a spatial axis by using a streak camera. The temporal shearing process and the spatio temporal integration process are denoted by operators $\boldsymbol{S}$ and $\boldsymbol{T}$, respectively. As a result, the observed image is mathematically formulated as

$$\boldsymbol{E} = \boldsymbol{TSCI}.$$

B. Image Restoration Process

An overview of the restoration process in N-CUP method is shown in Fig. 2. We repeatedly perform CUP method [11]

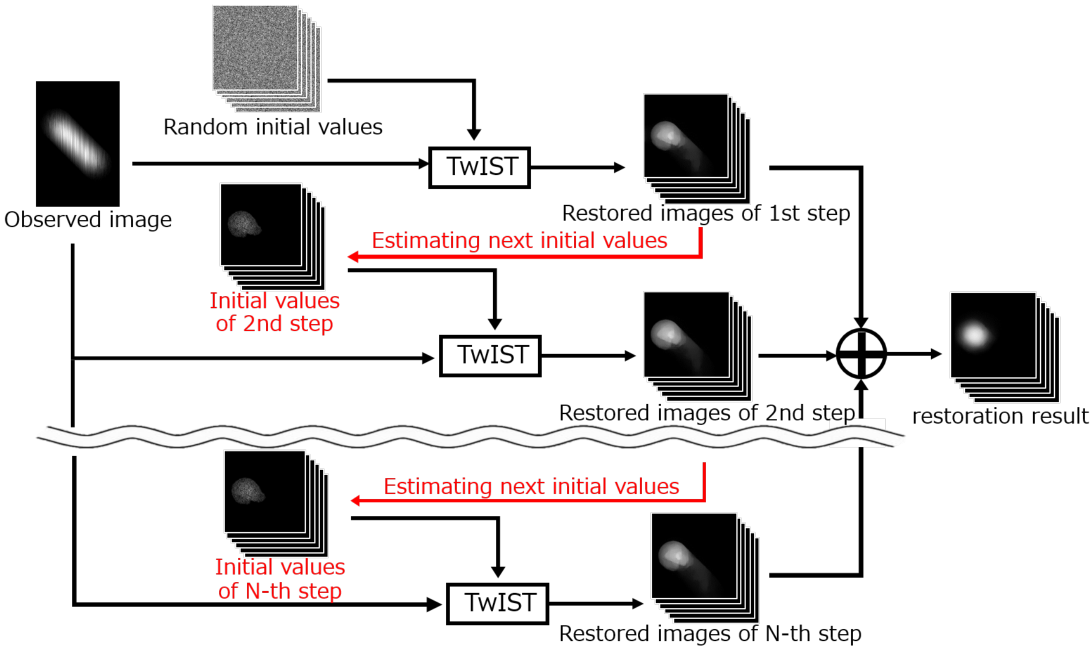

Fig. 2. Overview of the restoration process in N-CUP method.

while estimating the reliability of the restoration results; then, we obtain the final restoration result on the basis of the estimated reliabilities.

In each step of N-CUP method, we estimate the target phenomenon $\boldsymbol{I}$ by minimizing the following objective function:

$$F = \frac{1}{2}\|\boldsymbol{E} - \boldsymbol{TSCI}\|^2 + \tau\Phi(\boldsymbol{I}). \quad (1)$$

Here, τ is a regularization parameter and $\Phi(\boldsymbol{I})$ is the regularization function in the form of total variation (TV) [11], which is shown as follows:

$$\begin{aligned}\Phi(\boldsymbol{I}) = &\sum_{t=0}^{N_{t-1}} \sum_{i=1}^{N_x \times N_y} \sqrt{(\Delta_i^h \boldsymbol{I}_t)^2 + (\Delta_i^v \boldsymbol{I}_t)^2} \\ &+ \sum_{x=1}^{N_x} \sum_{i=1}^{N_y \times N_t} \sqrt{(\Delta_i^h \boldsymbol{I}_x)^2 + (\Delta_i^v \boldsymbol{I}_x)^2} \\ &+ \sum_{y=1}^{N_y} \sum_{i=1}^{N_x \times N_t} \sqrt{(\Delta_i^h \boldsymbol{I}_y)^2 + (\Delta_i^v \boldsymbol{I}_y)^2}\end{aligned}$$

Here, $\boldsymbol{I}_x, \boldsymbol{I}_y, \boldsymbol{I}_t$ denote the 2D lattices along the dimensions x, y, t. Δ_i^h and Δ_i^v are horizontal and vertical first-order local difference operators on a 2D lattice. The above optimization problem can be solved by using TwIST algorithm [12]. Concretely, the following equations are iteratively calculated:

$$\boldsymbol{I}_1 = \Gamma_{\frac{2}{\tau}}(\boldsymbol{I}_0),$$

$$\boldsymbol{I}_{t+1} = (1-\alpha)\boldsymbol{I}_{t-1} + (\alpha - \beta)\boldsymbol{I}_t + \beta\Gamma_{\frac{2}{\tau}}(\boldsymbol{I}_t).$$

Here, α and β are predefined parameters and $\Gamma_{\frac{2}{\tau}}$ is defined as

$$\Gamma_{\frac{2}{\tau}}(\boldsymbol{I}) = \Psi_{\frac{2}{\tau}}(\boldsymbol{I} + (\boldsymbol{TSC})^T(\boldsymbol{E} - \boldsymbol{TSCI})).$$

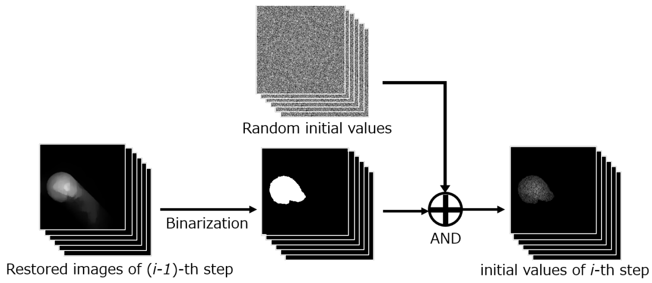

Fig. 3. Scheme of estimating initial values of i-th $(= 2, 3, \cdots, N)$ step in N-CUP method.

Here, $\Psi_{\frac{2}{\tau}}$ represents a denoising operation defined as

$$\Psi_{\frac{2}{\tau}}(\boldsymbol{x}) = \arg\min_{\boldsymbol{x}}\{\frac{1}{2}\|\boldsymbol{x} - \boldsymbol{y}\|^2 + \frac{2}{\tau}\Phi(\boldsymbol{x})\},$$

where $\boldsymbol{x}$ and $\boldsymbol{y}$ represent an original image and a noisy observation, respectively.

In the first step of N-CUP method, $\boldsymbol{I}_0$ is initialized with the random values. Then the initial values of the subsequent steps are determined by using the restored images $\boldsymbol{I}$ in the previous step (see Fig. 3). Concretely, the restored images are first binarized using a threshold calculated by linear discriminant analysis (LDA) [13] to separate the phenomenon and artefacts. LDA determines a threshold that separates samples into two classes. The separation is defined as the ratio of the variance

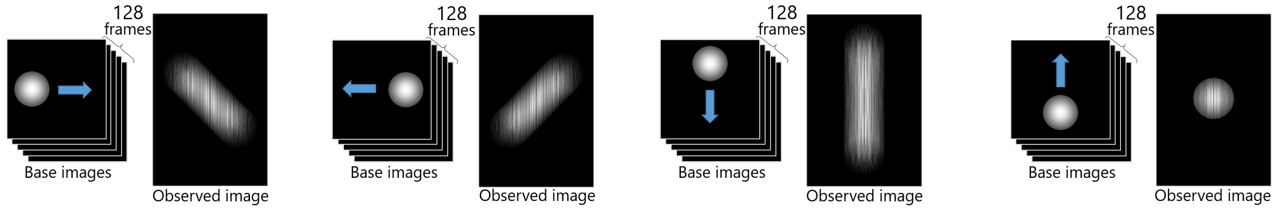

(a) From left to right (b) From right to left (c) From top to bottom (d) From bottom to top

Fig. 4. Image datasets emulating phenomena of fundamental light emissions.

between the classes to the variance within the classes:

$$\begin{aligned} S &= \frac{\sigma^2_{between}}{\sigma^2_{within}} \\ &= \frac{n_1(\mu_1 - \mu_t)^2 + n_2(\mu_2 - \mu_t)^2}{n_1\sigma_1^2 + n_2\sigma_2^2}. \end{aligned}$$

Here, n_1, μ_1 and σ_1 are the numbers of pixels, mean and variance of the class that is lower than a threshold. n_2, μ_2 and σ_2 are the numbers of pixels, mean and variance of the class that is higher than threshold. μ_t is mean of all pixel values in an image. Next, the binarized phenomenon and the random values are integrated. It should be noted that the integrated values have information of the shape of the phenomenon. Therefore, by using the integrated values as initial values of the optimization in the next step, we can accurately estimate the target phenomenon.

Finally, the restored images $\boldsymbol{I}$ of each step are fused based on the reliabilities. The reliabilities of each restoration result are defined as the inverse of the value of objective function F in Eq. (1) when the objective function has been minimized. In this paper, the restored images with maximum reliability are adopted as the final restoration result. Thus, we can successfully realize the image restoration.

III. Experimental Results

In this section, we show experimental results to verify the performance of N-CUP method. We emulated phenomena of fundamental light emissions and constructed simulated image datasets. Figure 4 illustrates the constructed image datasets. In this simulation, the observed image contains 128 base images. Similar to the conventional method [11], base images are encoded with random binary pattern and then each base image is shifted by a pixel in the space along the vertical direction relative to the previous image. Then all base images are projected on one plane and form a 2D image. In the image datasets, the phenomena have same shape but move different directions since we aim to verify the robustness of N-CUP method for the direction of the motion.

To evaluate image restoration quality, Structural Similarity (SSIM) [14] and Peak Signal-to-Noise Ratio (PSNR) [15] are used. The larger SSIM and PSNR values are, the higher image restoration quality is. The regularization parameter τ was set to one that gave the best SSIM value in $[2^{-3}, 2^{-2}, 2^{-1}, 2^0, 2^1, 2^2, 2^3]$.

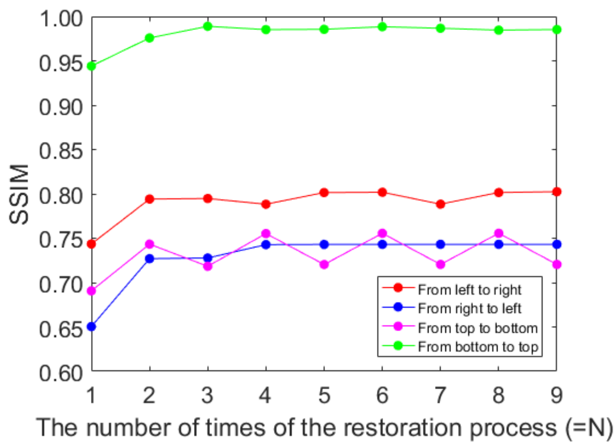

Fig. 5. Relationship between the number of times of the restoration process ($= N$) and SSIM in N-CUP method.

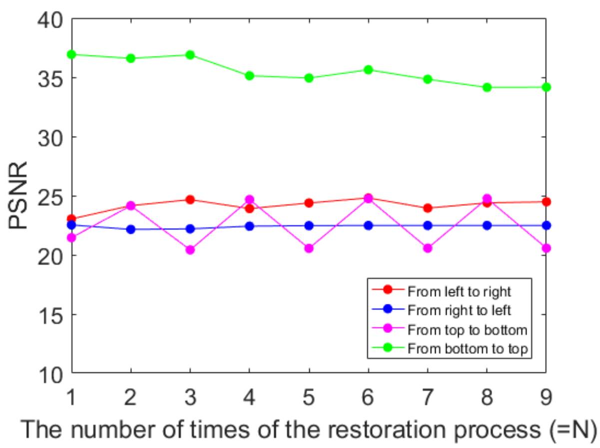

Fig. 6. Relationship between the number of times of the restoration process ($= N$) and PSNR in N-CUP method.

Figures 5 and 6 show the relationship between the number of times of the restoration process ($= N$) and SSIM and PSNR, respectively. We defined the number of iterations as nine since we can see that the restoration result was converged. From these figures, it can be seen that the restoration accuracy changed according to the iterations. Therefore, we can confirm

TABLE I. Quantitative evaluations of restoration results by the following methods:
(a) Conventional method (CUP method) [11],
(b) Method that adopts restored images in the final step of N-CUP method,
(c) Method that adopts weighted mean of inverses of F in Eq. (1) in each step of N-CUP method as the reliability,
(d) N-CUP method (the proposed method).

	SSIM				PSNR			
	(a)	(b)	(c)	(d)	(a)	(b)	(c)	(d)
From left to right	0.744	**0.802**	0.793	**0.802**	23.03	24.47	24.47	**24.80**
From right to left	0.650	**0.743**	0.732	**0.743**	**22.52**	22.48	22.48	22.48
From top to bottom	0.691	0.721	0.730	**0.756**	21.45	20.56	20.56	**24.75**
From bottom to top	0.944	0.985	0.983	**0.989**	**36.92**	34.15	34.15	36.88
Average	0.757	0.813	0.810	**0.823**	25.98	25.42	25.42	**27.23**

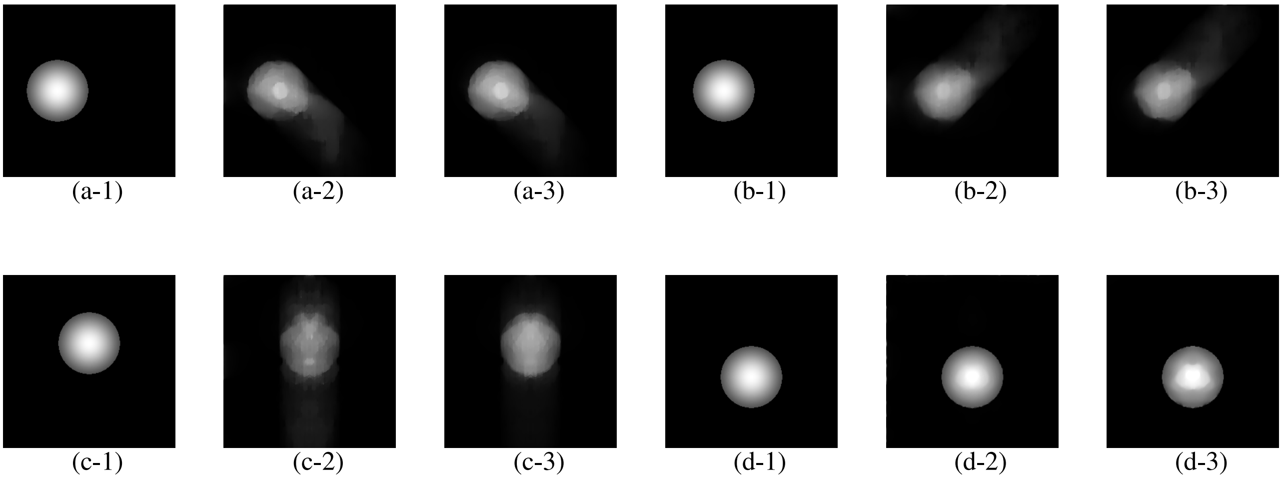

Fig. 7. For a case where a phenomenon moves from left to right, (a-1), (a-2) and (a-3) show the ground truth, restoration results by CUP method [11] and our N-CUP method, respectively. For a case where a phenomenon moves from right to left, (b-1), (b-2) and (b-3) show the ground truth, restoration results by CUP method [11] and our N-CUP method, respectively. For a case where a phenomenon moves from top to bottom, (c-1), (c-2) and (c-3) show the ground truth, restoration results by CUP method [11] and our N-CUP method, respectively. For a case where a phenomenon moves from bottom to top, (d-1), (d-2) and (d-3) show the ground truth, restoration results by CUP method [11] and our N-CUP method, respectively.

that it is necessary to suitably fuse the multiple results for accurate restoration.

To verify the suitable fusion method, we compare other fusion methods. One is a method that adopts the restored images in the final step. The other is a method that adopts the weighted mean of the inverse of F shown in Eq. (1) of each step. The restoration results by these fusion method are shown in Table I. From this table, we can see that N-CUP method that adopts the restored images with maximum reliability provides the highest performance. In comparison with conventional method [11], our proposed method increased SSIM from 0.757 to 0.823. Also, PSNR increased from 25.98 to 27.23.

An example of the restoration results are shown in Fig. 7. In Fig. 7 (a), we can see that the artefact can be reduced by N-CUP method. Furthermore, in Figs. 7 (a), (b) and (c), we can see that the contour of phenomenon is sharper than the conventional method [11]. In conclusion of the experimental results, we confirmed that the results of N-CUP method are quantitatively and qualitatively superior than those by comparative methods.

IV. CONCLUSION

In this paper, we proposed N-CUP method that restores minute light emissions from an image observed by a streak camera. In the conventional method called CUP method, there was a case in which artefacts occur in the restoration results depending on initial values of the optimization for restoration. Our proposed N-CUP method overcame this limitation by iteratively performing CUP method while estimating initial values suitable for the optimization. Through simulation using image datasets emulating phenomena of fundamental light emissions, it was confirmed that N-CUP method obtained more successful restoration results than those by comparative methods.

ACKNOWLEDGMENT

This work was partly supported by JSPS KAKENHI Grant Number JP18H01193.

REFERENCES

[1] O. Munn and A. Beach, "A horse's motion scientifically determined," *Scientific American*, vol. 39, no. 16, p. 241, 1878.

[2] B. Heshmat, G. Satat, C. Barsi, and R. Raskar, "Single-shot ultrafast imaging using parallax-free alignment with a tilted lenslet array," in *CLEO: 2014*, p. STu3E.7.

[3] Y. Kondo, K. Takubo, H. Tominaga, R. Hirose *et al.*, "Development of "hypervision hpv-x" high-speed video camera," *Shimadzu Rev*, vol. 69, pp. 285–291, 2012.

[4] W. Lauterborn, "High-speed photography of laser-induced breakdown in liquids," *Applied Physics Letters*, vol. 21, no. 1, pp. 27–29, 1972.

[5] E. Dianov, V. Fortov, I. Bufetov, V. Efremov *et al.*, "High-speed photography, spectra, and temperature of optical discharge in silica-based fibers," *IEEE Photonics Technology Letters*, vol. 18, no. 6, pp. 752–754, 2006.

[6] S. Thoroddsen, T. Etoh, and K. Takehara, "High-speed imaging of drops and bubbles," *Annual Review of Fluid Mechanics*, vol. 40, no. 1, pp. 257–285, 2008.

[7] A. Velten, E. Lawson, A. Bardagjy, M. Bawendi *et al.*, "Slow art with a trillion frames per second camera," in *Proceedings of SIGGRAPH*, 2011, p. 44.

[8] A. Velten, T. Willwacher, O. Gupta, A. Veeraraghavan *et al.*, "Recovering three-dimensional shape around a corner using ultrafast time-of-flight imaging," *Nature Communications*, vol. 3, pp. 745:1–745:8, 2012.

[9] Z. Li, R. Zgadzaj, X. Wang, Y.-Y. Chang *et al.*, "Single-shot tomographic movies of evolving light-velocity objects," *Nature Communications*, vol. 5, pp. 3085:1–3085:12, 2014.

[10] K. Nakagawa, A. Iwasaki, Y. Oishi, R. Horisaki *et al.*, "Sequentially timed all-optical mapping photography (stamp)," *Nature Photonics*, vol. 8, pp. 695–700, 2014.

[11] L. Gao, J. Liang, C. Li, and L. V. Wang, "Single-shot compressed ultrafast photography at one hundred billion frames per second," *Nature*, vol. 516, pp. 74–77, 2014.

[12] J. M. Bioucas-Dias and M. A. Figueiredo, "A new twist: Two-step iterative shrinkage/thresholding algorithms for image restoration," *IEEE Transactions on Image Processing*, vol. 16, no. 12, pp. 2992–3004, 2007.

[13] N. Otsu, "An autmatic threshold selection method based on discriminant and least squares criteria," *The Transactions of the Institute of Electronics, Information and Communication Engineers D*, vol. 63, no. 4, pp. 349–356, 1980.

[14] Z. Wang, A. C. Bovik, H. R. Sheikh, E. P. Simoncelli *et al.*, "Image quality assessment: from error visibility to structural similarity," *IEEE Transactions on Image Processing*, vol. 13, no. 4, pp. 600–612, 2004.

[15] S. H. Chan, R. Khoshabeh, K. B. Gibson, P. E. Gill *et al.*, "An augmented lagrangian method for total variation video restoration," *IEEE Transactions on Image Processing*, vol. 20, no. 11, pp. 3097–3111, 2011.